18TH WORLD CONFERENCE ON EARTHQUAKE ENGINEERING
WCEE2024
MILAN

MILAN, ITALY
30TH JUNE - 5TH JULY 2024
www.wcee2024.it

DAMAGE STATES OF STRUCTURAL SILICONE GLAZED FACADES

S. Bianchi[1], V. Hayez [2], G. Lori[3], M. Overend[1], G. Manara[3]

[1] Delft University of Technology, Delft, The Netherlands, s.bianchi@tudelft.nl

[2] Dow Silicones, Seneffe, Belgium

[3] Permasteelisa S.p.A., Vittorio Veneto, Italy

Abstract: *Unitized curtain walls play an integral role in contemporary architectural designs, offering advantages such as lightweight construction, high quality control and ease of installation. However, recent post-earthquake surveys have revealed their vulnerability to damage, raising concerns about potential hazards in post-earthquake scenarios. Even slight-to-moderate damage can lead to loss of functionality and economic losses, arising from breaches in the air/water tightness of the building envelope and costly repairs/replacement. Furthermore, as the damage progresses from moderate to severe, it poses a life-threatening risk to occupants and pedestrians due to falling glass or debris from the damaged façade. Among the different types of unitized curtain walls, structural silicone glazing emerges as a resilient assembly system with the potential to enhance the seismic performance of the façade. Nevertheless, despite initial studies on the seismic behaviour of the silicone bonding sealant, research in this field remains limited. Typically, experimental investigations overlook the analysis of the complete sequence of damage states and the ultimate resistance of the various components within the silicone-bonded façade. As part of a broader EU-funded research project, this paper presents the key findings derived from an experimental campaign on structural silicone glazed facades conducted at the Permasteelisa Group laboratory. The overall research aimed to gather information on the post-earthquake functionality and the failure modes of alternative façade designs. The hierarchy of damage mechanisms that occur during an earthquake was established by testing full scale façade prototypes with different pane and silicone joint dimensions, frame displacement capacity and loading mode. The testing procedure involved a series of in-plane displacement-controlled crescendo tests, time histories and monotonic testing, gradually increasing the intensity levels to evaluate the progressive damage states within the façade system. The paper provides the main outcomes derived from both damage observations and data post-processing, including the assessment of utilization factors and fragility curves for the façade components. These results offer valuable insights into the seismic behaviour of structural silicone glazed facades, thereby supporting the future development of design guidelines and practices for more resilient facade systems.*

1. Introduction

Past earthquakes have highlighted the vulnerability of glazed curtain walls, thus leading to a growing effort to design them to withstand seismic actions. Glazed facades are directly impacted by earthquakes, experiencing inter-storey drift ratios, displacement incompatibilities and inertia forces. Seismic movements can initially be sustained by the facade through internal gaps and deformations, then, as deformations become larger, specific parts of the system may experience concentrated stresses and subsequent damage. Typical damage mechanisms observed after earthquakes include: (a) gasket degradation, leading to air and/or water

infiltrations; (b) glass fracture, which may not immediately cause human injury but is a source of further air permeability, water infiltration and other indirect damages; (c) glass fallout, posing potential injury / loss-of-life risks and causing substantial economic consequences (Miranda et al. 2010, Baird et al. 2011). This potential damage (Figure 1a) raises two major concerns regarding the façade performance during and after a seismic event: (a) hazard to people: shattered storefronts and elevated glazed systems pose threats to individuals, potentially resulting in injuries and fatalities at street level; (b) building downtime and repair costs: the restoration of operations and services to normalcy can be hindered by a compromised building envelope due to damage to glazing systems.

In this context Structural Sealant Glazing (SSG) systems are typically considered to outperform other glazing systems acknowledged. This is supported by fragility data collected and analysed from experimental testing. For example, Figure 1b illustrates a comparison in terms of the probability of glass fracture between dry-glazed (with rubber gaskets and mechanical restraints) and wet-glazed systems (employing structural silicone). This data demonstrates the SSG solution is able to withstand higher seismic demand before achieving the same damage condition. Current building codes therefore provide guidelines for properly sizing structural silicone joints, being the design crucial for enhancing structural performance. If the glass curtain wall lacks specially designed connections to isolate it from the building frame and accommodate relative motion, the seismic racking motion of the building frame will place substantial demands on the integrity of the sealant that secures the glass to the curtain wall framing (Zarghamee et al. 1996).

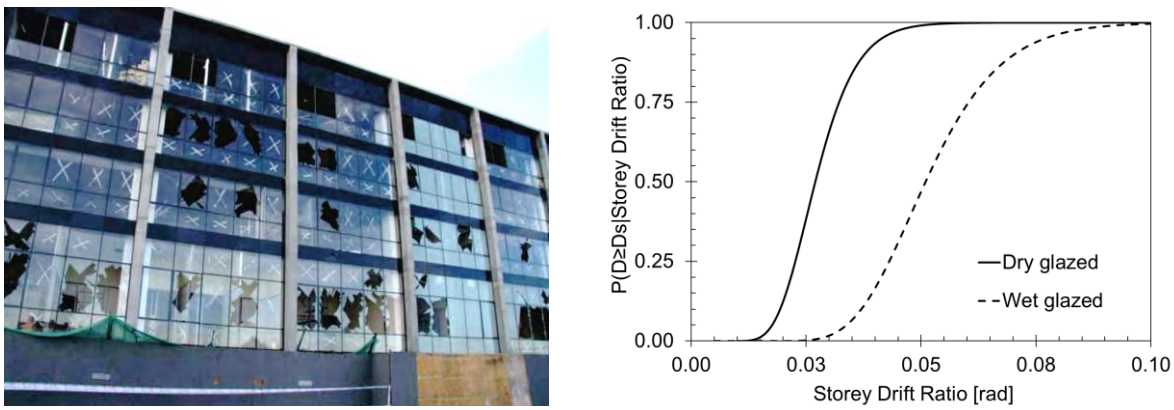

(a) (b)

Figure 1. (a) Glazing damage observed after Chile 2010 earthquake (Miranda et al. 2010); (b) Fragility curves for glass cracking of a dry vs. wet glazed system (data elaborated from Memari et al. 2011).

Numerous experimental studies have been conducted to assess the seismic performance of glazing systems over the past few decades, as discussed in the review papers by Huang et al. (2017) and Bianchi and Pampanin (2022). These studies have primarily focused on investigating the movement and drift capacity of glass panels by means of in-plane monotonic and cyclic racking testing, bi-directional tests, or shake table testing (e.g., Memari et al. 2011, Broker et al. 2012, Lu et al. 2016). Their objectives include studying the influence of different glass types, clearance values and connection systems, as well as identifying damage patterns and analysing in-plane/out-of-plane actions. Additionally, recent experimental tests conducted by Arifin et al. (2020) and Bianchi et al. (2022) have focused on studying the post-earthquake serviceability of glazed curtain walls, particularly in terms of water and air tightness.

In parallel with experimental testing, recent research has emphasized the use of finite element analysis (FEA) simulations to study the façade behaviour. While some studies have focused on numerical investigations of the entire façade systems (e.g., Memari 2011, Ciurlanti et al. 2023), there is a growing trend towards more refined modelling of silicone behaviour to accurately capture the response of SSG systems (Nuñez Enriquez 2022, Kimberlain et al. 2022). These studies have successfully used a Mooney Rivlin hyperelastic material model to capture the nonlinear response of structural sealant joints in seismic drift tests. The simulation and testing of façade connections or entire façade systems have confirmed the importance of evaluating the seismic performance of SSG joints based on the façade layout and bonding configuration. With a strong correlation between FEA simulation and full-scale seismic testing, these investigations have confirmed that

simulation-based calculations can effectively predict sealant performance in seismic tests. This approach allows for a more efficient assessment of the seismic performance of façade systems before conducting costly validation tests. Consequently, there is a pressing need for extensive research on the seismic performance of SSG, involving experimental analysis of different sample configurations and the creation of finite element models to replicate the behaviour of the tested samples (Hayez et al. 2023).

As part of an EU-funded research project, SAFE-FACE, led by Delft University of Technology and Permasteelisa Group, the seismic behaviour of SGG façade systems has been investigated to address this need. The overarching goal of the project is to comprehensively examine the seismic performance of full-scale unitized curtain walls from a multi-performance perspective, encompassing both serviceability performance and the ultimate limit state of alternative facade designs through an extensive research program. The tests involve diverse facade configurations, including dry glazing (DG) and structural sealant glazing (SSG) systems, with different construction details. This paper specifically presents the experimental results for SSG facade systems featuring various structural silicone aspect ratios. By means of data postprocessing and observations, the focus is on assessing expected damage mechanisms resulting from layout variations and identify the sequence of damage states occurring with increasing levels of seismic shaking.

2. Research method

A comprehensive experimental campaign was conducted at the Permasteelisa Group laboratory in Vittorio Veneto, Italy (Bianchi et al. 2022). The key objectives of the research were: (a) to assess how various facade details, such as dry *vs.* wet systems, joint dimensions and the types of glass and frames, affect the seismic performance of full-scale unitized curtain wall systems; (b) to calibrate finite element numerical models that can accurately depict both local (joint/connection) responses and global (facade) behaviours, thus validating and enhancing existing numerical modelling procedures; (c) to investigate the damage mechanisms of the facades, including non-seismic responses such as air leakage, water penetration and wind resistance, along with examining ultimate failure modes. In order to achieve these objectives, a series of experiments was carried out, involving both quasi-static (monotonic) and dynamic testing (including sinusoidal and real earthquake signals) on various specimen configurations. Furthermore, seismic tests were combined with serviceability tests at lower seismic intensities to gather crucial insights into the maximum seismic levels that the facade can withstand before experiencing functionality loss and structural failure.

This paper primarily focuses on the final phase of experimental testing, which aimed to evaluate the seismic performance of SSG façade systems, for their earthquake resilience. They indeed effectively prevent glass fracture during small to moderate earthquakes by securely connecting the glass panel to the frame using a structural sealant joint, thereby reducing the risk of hard contact between the glass and metal surfaces. In contrast, a dry glazed system with mechanical caps can lead to glass fracture when subjected to inter-storey drifts, as they introduce local contact hard-spots and lack the continuous attachment found in SSG systems. Furthermore, SSG systems can retain broken glass, particularly when laminated glass is used and structural joint integrity is maintained. However, correct joint dimensions are critical to fully harness the benefits of the system and effectively transfer seismic forces to accommodate imposed movements. Depending on the adhesive properties and joint dimensions, SSG systems can meet seismic performance requirements associated with various damage levels.

Therefore, experimental tests were conducted on facade specimens featuring varying joint dimensions and frame characteristics, including both flexible and rigid frames. The aim was to experimentally examine the performance of different units. These experimental results can be compared with appropriately developed numerical models for the tested specimens for getting more insights on the local behaviour (Hayez et al. 2023). This paper primarily focuses on presenting the outcomes of the experiments. It offers an overview of the key findings derived from observations and data post-processing, particularly in terms of how joint dimensioning impacts façade movements and the potential mechanisms of damage.

3. Experiment design

3.1. Specimen configurations

Two types of facade units were available for seismic testing, differing in their total height and glass/spandrel dimensions (Figure 2a). These units consist of double glazing units bonded to an aluminium frame (type 6063

T6) by SSG joints. Along mullions and transoms, the panels are equipped with stack joints that have sufficient clearance to ensure free accommodation of any movement that the building structure may undergo. The connection system to the main structure involves the use of hooks, brackets and adjusting bolts. The starter sill is connected to the bottom transom of the units through screwed alignment blocks and shear keys. Each unit generally requires two hooks for the upper anchorage to the structure. These hooks have different constraints in the horizontal in-plane direction: one hook is fixed using screws, while the other hook is free to move. This constraint scheme is applied to allow the unit to accommodate differential thermal and building movements. Additionally, the hooking connections can also accommodate construction tolerances. Vertical tolerance is achieved through the adjusting bolts, while horizontal tolerance is provided by the clearance between the hook and the steel plate.

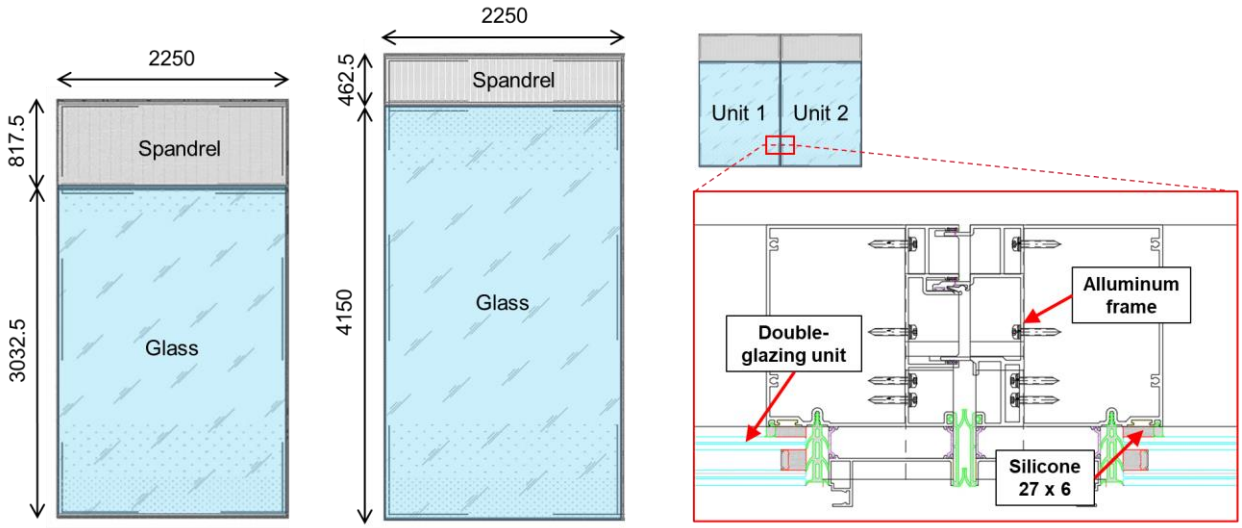

Figure 2. Dimensions of the units (in mm) and joint detailing.

The original SSG units embedded DOWSIL™ 993 structural glazing silicone with dimensions of 27mm bite and 9mm thickness for both mullions and transoms, as shown in Figure 2b. As part of the research objectives, the design of these units was modified by reglazing them to introduce variations in the joint design, in order to increase the likelihood of failure during the seismic testing. The choice of silicone dimensions indeed enabled to investigate the potential influence of the joint aspect ratio, given that lower aspect ratios can enhance the movement capability and influence the hierarchy of damage among the different components in the facade system. Four different joint dimensions were thus identified, as summarized in Table 1, by means of initial simplified numerical modelling and predictions of the façade units' seismic behaviour. The numerical analysis aimed at defining which units were most susceptible to failure, based on the type of seismic loading (monotonic vs. dynamic), the glass panel dimensions and the frame's movement capability (rigid vs. flexible), as described by Hayez et al. (2023).

Table 1. Summary of façade unit and joint dimensions (in mm) and expected behaviour.

ID	Unit	Joint	Description
U1	2250 x 4150	27 x 9	Design, unit aspect ratio of 1.8, silicone aspect ratio of 3
U2	2250 x 4150	9 x 9	Variation 1, unit aspect ratio of 1.8, silicone aspect ratio of 1
U3	2250 x 3850	20 x 9	Variation 2, unit aspect ratio of 1.7, silicone aspect ratio of 2.2
U4	2250 x 3850	9 x 9	Variation 3, unit aspect ratio of 1.7, silicone aspect ratio of 1

3.2. Test setup

The experimental testing was conducted at the Permasteelisa laboratory in Vittorio Veneto, Italy, which is equipped to test full-scale facades with dimensions of up to approximately 10 meters in width and height. These specimens can be mounted on a two-story steel support structure, characterized by a seismic "blue" beam. A hydraulic actuator is employed to apply to this beam a maximum displacement of ± 75 mm in the

horizontal (X) in-plane and ± 50 mm in the vertical (Y) direction. This actuator is integrated with a digital controller and a control panel to facilitate the application of the desired displacement, both quasi-static and dynamic loading sequences. The specimens can be tested in two different layouts. Layout L1, designed for testing single-story glazed units or units arranged in a row. This layout enables the analysis and comparison of the behavior of various facade systems. Layout L2, intended for testing facades spanning two levels. While L2 may not replicate real-world scenarios where different inter-story drift ratios occur at distinct floor levels, it is commonly employed in performance tests to analyze the movement of the facade at the horizontal joint and ensure compliance with project requirements. Based on the initial blind predictions, various specimen configurations were considered encompassing both L1 and L2 layouts (Figure 3). This paper specifically focuses on providing main outcomes obtained for configurations 1 and 2 as highlighted in the figure.

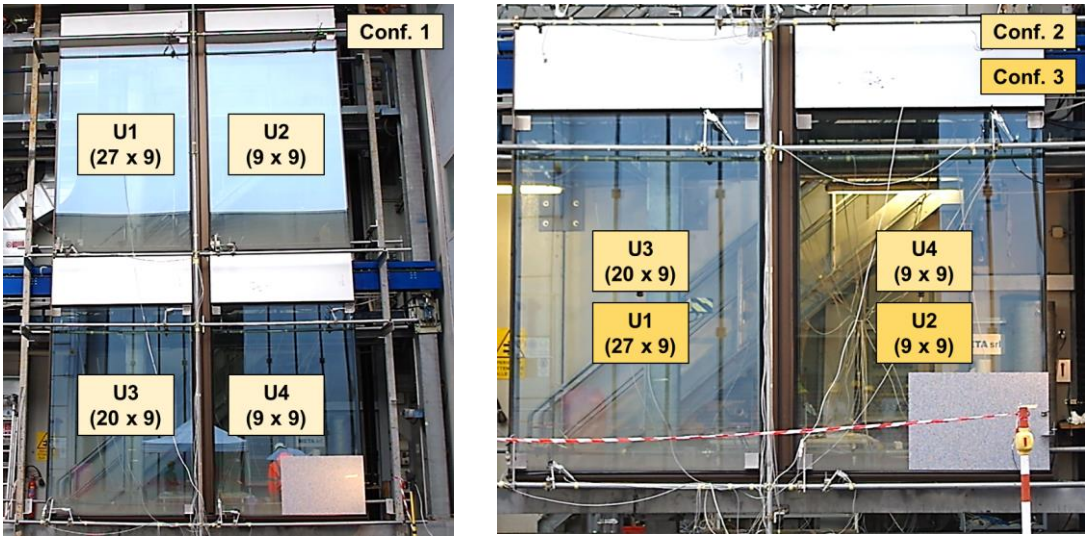

(a) (b)

Figure 3. Specimen configurations: four units in L2 layout (a), two units in L1 layout (b).

An instrumentation layout was carefully devised for each configuration to capture both the in-plane and out-of-plane movements of the facade under horizontal and vertical loading conditions. The comprehensive monitoring system consisted of a total of 31 displacement sensors, which included potentiometers and linear transducers with strokes of 50mm, 100mm and 200mm. These sensors were employed to record both the vertical and horizontal displacements of the glass panels and framing system, including the hook/bracket connections to the seismic beam. Furthermore, draw wires with a 50mm measurement range were utilized to monitor the diagonal and corner elongations of the internal frame. Laser sensors with detection capabilities of 200mm or 500mm were implemented to track the movement of the seismic beam. Furthermore, accelerometers were placed to measure accelerations on the glass panels and bracket connections, while strain gauges were used to record strains on the glass, specifically in the vicinity of the setting blocks, as well as on a bottom mullion/transom joint of the frame system.

Since only the external mullions were accessible for visual monitoring, a total of five cameras (including GoPro and digital cameras) were positioned to capture the entire length of the silicone joint in the 9x9mm² unit. Once the silicone joint failure was reached, the cameras were repositioned to focus on the mullion of the other unit (20x9mm² or 27x9mm²). Adhesive rulers were affixed along the perimeter zone to facilitate the monitoring of relative movements in the silicone. Furthermore, laser sensors were installed in the bottom corner to monitor relative displacements between the glass and frame in both the horizontal and vertical directions. To track the potential propagation of the crack in the silicone, visual monitoring was conducted, and measurements were taken with rulers to capture any increase in crack size. In addition to the visual monitoring of the edge, an extra camera was positioned in front of the test setup to capture the overall behavior of the unit.

The testing protocol comprised various types of tests, as illustrated in Figure 4, with the objective of inducing failure in the silicone joints through dynamic or monotonic seismic loading. Initially, dynamic tests were conducted on each specimen configuration using two primary approaches:

- Crescendo tests, following the AAMA 501.6 (2001) standard. These tests involved a gradual increase in the loading amplitude, ultimately reaching a maximum of 72mm displacement, determined by the test facility's capacity in the horizontal direction.
- Simulation of earthquake records, encompassing both far-field and near-fault scenarios, through inter-story drift time series. These time series were generated by performing non-linear numerical analysis on a multi-story reinforced building (derived from the case study building in Bianchi et al. 2021) subjected to three different seismic events, which are summarized in Table 2. The earthquake records were thus scaled to achieve maximum drift amplitude levels of 24mm, 36mm and 72mm.

To maximize the capabilities of the laboratory and achieve higher drift values, quasi-static monotonic tests (horizontal in-plane) were carried out until reaching a maximum displacement of 225mm. After each loading step (every 25mm), testing was temporarily halted to allow for visual inspection of the silicone joint. Following the completion of unit testing, a full deglazing process was planned to determine the depth and location of any failures, if they occurred.

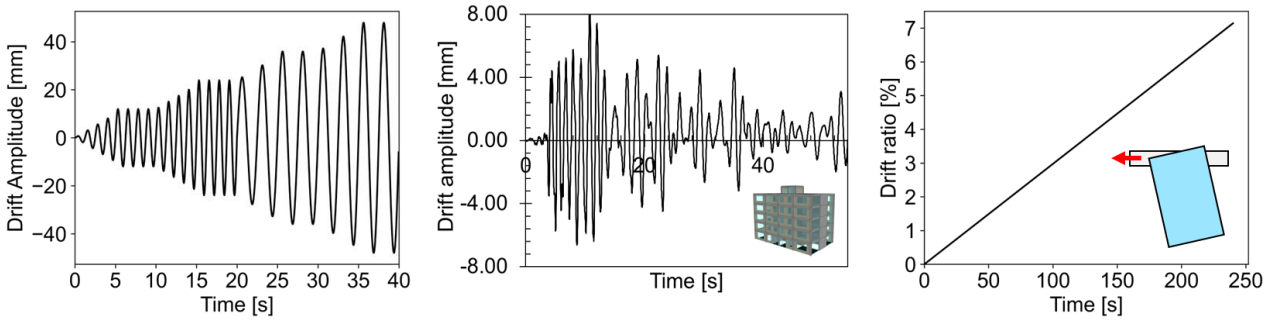

(a) (b) (c)

Figure 4. Type of seismic testing applied.

Table 2. List of selected records.

Event	Year	Magnitude Mw	Station ID	PGA [g]	Soil Type
Friuli	1976	6.0	ST33	0.11	C
Umbria-Marche	1997	6.0	ST223	0.17	C
Christchurch	2011	6.3	CCCC	0.17	D

4. Test results

4.1 Four-unit configuration

The initial experimental phase included dynamic testing of the specimen configuration comprising all four facade units connected to the two different floor levels. In this setup, the frame system was designed to withstand high drift amplitudes. To prevent the alignment screw from bearing on the starter sill profile and, consequently, to avoid horizontal sliding of the bottom transom at lower drift levels, an angular steel plate was introduced in the alignment screw connection. This design enhancement allows for greater relative vertical movement capacity of the bottom transom compared to the starter sill.

A series of tests, mono-directional (X) or bi-directional (XY) and including both Crescendo and earthquake tests, was conducted at two different intensity levels, with peak horizontal displacements of 24mm and 36mm. The facade units exhibited excellent performance during dynamic movements, demonstrating the effectiveness of the system's detailing. The in-plane differential seismic movements between floors, driven by inter-story drift, result in a racking motion characterized by rigid translation and rotation of the glass panels within the frame, which can undergo deformation. This leads to differential displacements between the glass and the frame, introducing stress into the SSG-joints due to these inter-story movements. The upward and

downward differential seismic movements are accommodated by the vertical stack joint along the transoms, designed with adequate vertical clearance.

This first experimental phase aimed to compare the performance of various units with differing glass and joint aspect ratios. It did not delve into investigating damage states within the facade system. The primary results, regarding the maximum horizontal and vertical movements experienced by the facade components, are presented in Table 3. These values were determined as averages of the maximum recorded displacements from both Crescendo tests and time-history experiments, considering horizontal direction and combined horizontal/vertical directions.

Table 3. Average displacement values recoded at the two earthquake intensities (Level 1 and 2).

	Horizontal Displacements									
	Glass				**Frame**				**Connection**	
	U1 27x9	U2 9x9	U3 20x9	U4 9x9	U1 27x9	U2 9x9	U3 20x9	U4 9x9	Bracket	Hook
Level 1 - 24mm	9.54	18.58	15.93	16.84	19.21	19.74	17.12	18.06	23.66	25.37
Level 2 - 36mm	15.2	28.89	25.58	27.26	30.22	31.08	25.42	27.39	36.00	38.17
	Vertical Displacements									
	Glass				**Frame**				**Connection**	
	U1 27x9	U2 9x9	U3 20x9	U4 9x9	U1 27x9	U2 9x9	U3 20x9	U4 9x9	Bracket	Hook
Level 1 - 24mm	9.08	5.38	5.37	4.60	4.18	5.31	5.81	9.40	-	4.56
Level 2 - 36mm	14.78	8.38	9.30	6.17	9.17	11.81	9.43	10.68	-	5.32

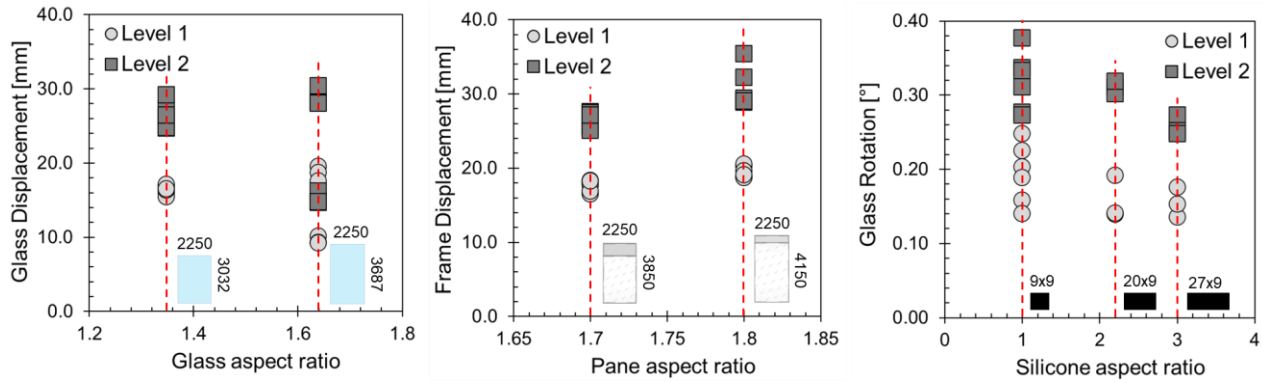

(a) (b) (c)

Figure 5. Effect of aspect ratio variations considering the experimental results from Level 1 (24mm) and Level 2 (36mm) testing.

By elaborating on the experimental data, the impact of joint and unit aspect ratio variations on façade movements (displacements and rotations) can be highlighted, as shown in Figure 5. The key observations are as follows: (i) horizontal glass displacement is significantly influenced by the silicone dimensions, especially at higher aspect ratio (comparing 9x9 vs. 27x9 configurations), resulting in a notable dispersion in the results; (ii) considering the overall unit aspect ratio, frame displacements increase at higher aspect ratios with less data dispersion, resulting in a maximum frame diagonal elongation of approximately 3.2mm; (iii) glass rotation decreases with increasing silicone aspect ratio, with more data dispersion at lower aspect ratios due to the influence of glass and unit dimensions on the results. Analyzing the results from earthquake records, similar outcomes were observed for both Far Field inputs (Friuli and Umbria-Marche), while higher displacements were recorded for the Near Fault record (Christchurch) due to the involved frequency range.

In addition to recording facade movements in terms of displacements and rotations, acceleration values were also measured at the center of the glass panels for both the 20x9 and 27x9 units, as well as at the bracket connections. Focusing on the earthquake records, it was observed a maximum amplification factor in the range of 1.2-1.3 for both units due the components' inherent resilience and flexibility of the frame system. The amplification factor was calculated by comparing the recorded glass acceleration with the acceleration at the bracket connected to the seismic beam. Furthermore, strain values were recorded in the different façade components to quantify utilization factors, representing the ratio of actual stress applied to the maximum stress the component can safely withstand. This test configuration included strain gauges in the following locations (Figure 5a): (i) bottom glass panels (U3 20x9, U4 9x9), positioned near the setting blocks where higher stresses are expected due to the panel's rotational behavior; (ii) frame system, in a corner on both the bottom transom and the vertical mullion; (iii) one of the brackets connected to the seismic beam. A filter was applied to the recorded strain data to eliminate noise outside the response range. Utilization factors were calculated assuming maximum strength values of 40MPa, 160MPa, and 355MPa for the glass, aluminum frame and steel brackets, respectively. The results indicated that both the glass and frame had utilization factors of less than 10% when investigating Levels 1 and 2 for this configuration, with the transom experiencing higher stress levels. In contrast, the bracket achieved a maximum utilization factor of 26% (Figure 5b), further affirming that its design is sensitive to the peak seismic force/acceleration values.

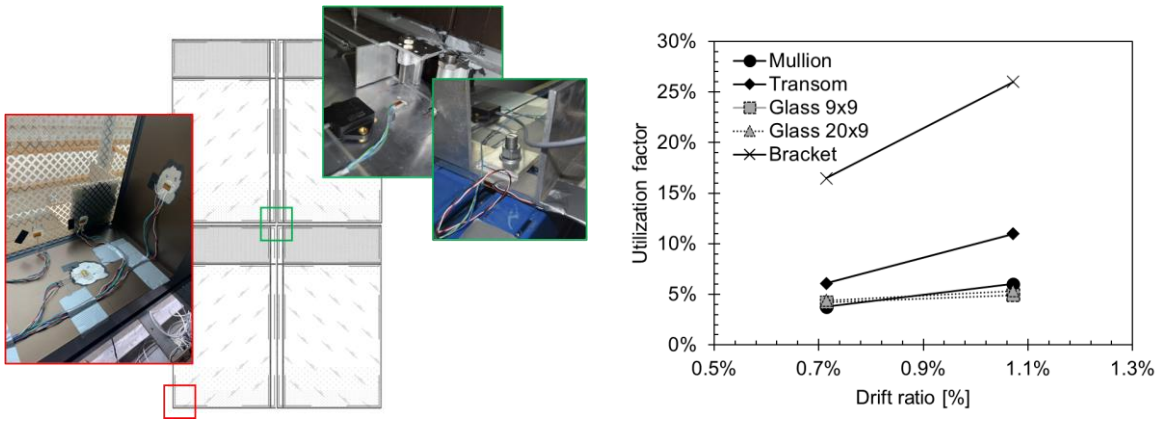

(a) (b)

Figure 5. (a) Location of strain gauges in the specimen. (b) Utilization factor of the different façade components at the two intensity levels.

No damage was observed in this configuration, primarily due to the maximum displacement achieved during lateral loading, which reached 72mm (equivalent to a drift ratio of [drift ratio value]). This value is below the threshold for structural damage to the facade. It's important to note that this test was conducted in isolation and not combined with non-seismic tests, so no investigation regarding serviceability loss related to air and water tightness was performed.

4.2 Two-unit configuration

The second testing phase involved the removal of units from the upper level to investigate the different damage states of the façade system with the U3 20x9 and U4 9x9 units. Multiple tests, including variations in the specimen configuration, were conducted as detailed below and summarized in Table 4.

First, the specimen was subjected to earthquake inputs, yielding data with similar displacements and rotation values when compared to the four-unit specimen at the same intensity levels. Subsequently, monotonic tests were conducted until reaching a maximum drift amplitude of 225 mm. During this sequence, damage to the silicone sheet between the two units was observed at 75 mm (equivalent to 2.2% drift value), followed by its failure at 100 mm (equivalent to 2.9% drift value). However, no further structural damage was observed due to the high displacement capabilities of the specimen. Results from the monotonic tests were analyzed in terms of displacements, up to the maximum capacity of the potentiometers, and in terms of strains. As expected, there was a significant reduction in strain values, given the absence of dynamic effects during this type of simulation. Particularly, utilization factors of less than 4% were observed for various components, representing values 3 and 2 times lower for the frame and glass, respectively, compared to when recorded during the

earthquake at the same intensity level. Notably, the bracket exhibited a 15-fold reduction in utilization factor. This outcome underscores the significant influence of acceleration at the bracket level, emphasizing its crucial role in design compared to displacement seismic demand.

Table 4. Testing sequence followed for the two-unit configuration.

N.	Type of Test	Description of Test	Unit 20x9	Unit 9x9	Visual inspection
1	Crescendo	Increasing displacement levels with peak value: 24 mm, 36 mm, 72 mm	Initial configuration	Initial configuration	-
2	Earthquake	Increasing displacement levels with peak value: 24 mm, 36 mm	Initial configuration	Initial configuration	-
3	Monotonic	Increasing displacement levels with peak value: 36 mm, 50 mm, 75 mm, 100 mm, 125 mm, 150 mm, 175 mm, 200 mm, 225 mm	Initial configuration	Initial configuration	Damage to the silicone sheet between units
4	Crescendo	Increasing displacement levels with peak value: 24 mm, 36 mm, 72 mm for each level of cracks in the silicone	Initial configuration	Artificially induced crack in the silicone (from 15mm to 300mm in the corner, then 20% along the full length)	-
5	Monotonic	Until a peak displacement of 200 mm	Frame fixed at the bottom transom	Artificially induced crack in the silicone (20% along the full mullion length)	Formation of cracks in the silicone of the 20x9 unit
6	Crescendo	Increasing displacement levels with peak value: 24 mm, 36 mm, 72 mm	Frame fixed at the bottom transom	Artificially induced crack in the silicone (20% along the full mullion length)	-
7	Monotonic	Until a peak displacement of 200 mm	Frame fixed at the bottom transom	Artificially induced crack in the silicone (20% along the full mullion length)	Detachment of glass in the corner for the 20x9 unit
8	Crescendo	Increasing displacement levels with peak value: 24 mm, 36 mm, 72 mm for each level of cracks in the silicone	Frame fixed at the bottom transom	Artificially induced crack in the silicone (from 20% to 80% cracking along the full perimeter)	-
9	Monotonic	Until a peak displacement of 200 mm	Frame fixed at the bottom transom	Artificially induced crack in the silicone (80% along the full perimeter)	-

After completing the initial testing sequence (1 to 3 in Table 4), a decision was made to create cuts in the silicone to simulate potential degradation caused by seismic events. The objective was to determine whether

a compromised silicone joint, visible through a crack, needed to be secured to mitigate the risk of collapse during potential aftershocks. Ideally, these cuts should have been applied in the area of highest strain, typically located at the top transom and corners of the glazed area for each sample. However, due to limited accessibility, cuts of increasing significance (ranging from 30 mm to 300 mm) were made along the free edge of the 9x9 unit. This modified configuration was subjected to Crescendo tests, with drift amplitudes reaching a maximum of 72 mm. Throughout the Crescendo series at each cut length, a consistent trend of increasing strain values and utilization factors was observed for all the different components. The maximum values reached approximately 20%, 4.5%, and 30% for the frame, glass and bracket, respectively. No propagation of artificially induced cracks was observed throughout the entire testing sequence.

To fully explore the specimen's behavior, the influence of the frame was assessed in the 20x9 unit. The original frame design was intended to accommodate seismic movements, preventing damage to the silicone joints. To investigate further, the frame was restrained at the bottom transom, preventing it from accommodating seismic movement through partial rotation. This modified configuration underwent a monotonic test with a maximum displacement of 200 mm. During this test, initial silicone damage was observed along the visible mullion at approximately 130 mm of drift amplitude (equivalent to a 3.8% drift level). At this point, the impact led to a 25% utilization factor in the glass. Following the silicone damage, a Crescendo test was repeated to assess the residual capacity of the silicone joint, which proved capable of supporting the glass throughout the test, ensuring life safety remained intact. Subsequently, a second monotonic test resulted in the complete detachment of the silicone joint in the bottom corner at 175 mm (equivalent to a 5.2% drift ratio).

(a) (b) (c)

Figure 6. Observed damage conditions: (a) failure of the silicone sheet between two units; (b) silicone damage along the mullion; (c) detachment of silicone joint in the corner.

When analyzing the results from the Crescendo tests conducted both before and after the silicone damage occurred (as depicted in Figure 6b), the recorded strain values revealed a notable shift in the hierarchy of strength among the various components. Prior to the silicone crack formation, the transom exhibited the highest utilization factor, followed by the mullion and the glass. However, once the crack had formed, this hierarchy underwent a significant change due to a substantial increase in strain in the glass panel, making it the second element with the highest utilization factor after the transom. This result is visually represented in Figure 7a, which displays the variation in utilization factors as a function of increasing levels of drift amplitude (24 mm, 36 mm, 48 mm, 60 mm, 72 mm).

In the case of the U4 9x9 unit, testing continued with both Crescendo and monotonic tests, but no further damage or crack propagation was observed within the unit, and the silicone remained stable throughout the testing process. An increase in stress in the glass was observed when comparing various 'degraded' configurations, characterized by increasing overall cracking along the perimeter. These configurations ranged from 20% cracking, simulated by applying 100 mm cuts along the perimeter, to 80% cracking, when the cracks reached a length of 400 mm. Although the application of this artificial damage to the silicone, the configuration remained stable throughout the test and the glass panel of the 9x9 unit experienced utilization factors below 10%, as depicted in Figure 7b.

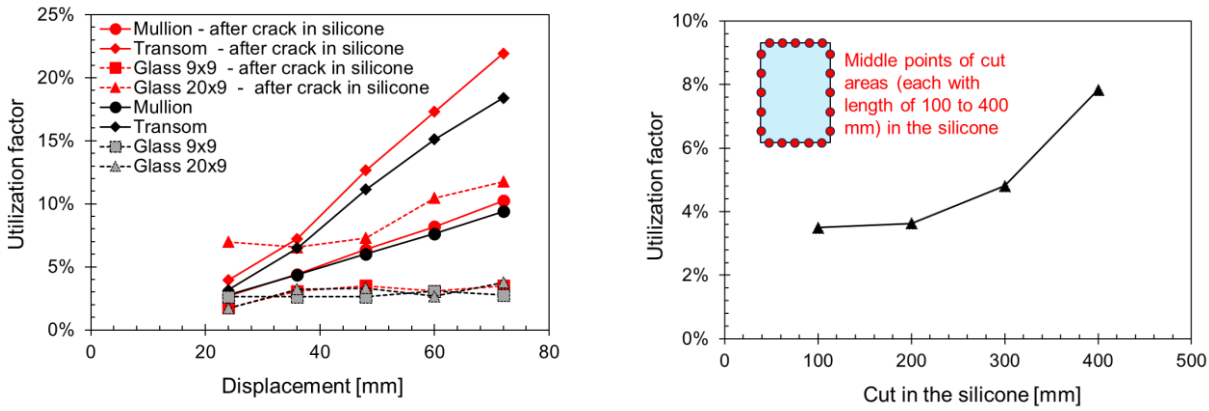

(a) (b)

Figure 7. (a) Unit 20x9: utilization factor during the Crescendo tests before and after the crack formed in the silicone. (b) Unit 9x9: variation of glass behaviour with increasing cuts in silicone.

4.3 Summary of damage states

The experimental tests have provided valuable insights into the damage states of SSG unitized curtain wall facades. It has been observed that the behavior of the frame system significantly influences the expected outcomes. When the frame is designed to withstand higher drift amplitudes, allowing for necessary vertical movements during seismic shaking, the failure mode of the system is primarily governed by the dislodgment of the façade from the bracket connections (as shown in the previous experimental phase described in Bianchi et al. 2022). Conversely, when the frame has limited displacement capacity, as simulated by fixing the bottom transom in the specimen configurations, the silicone experiences higher stress and may incur damage. Once cracking forms, the façade remains secure and retains the capacity to withstand additional shaking before reaching failure due to glass detachment at higher drift ratios. The observed potential damage states can be employed to generate 'tentative' fragility curves, by assuming a log normal distribution, in order to provide a direct comparison of the results, as illustrated in Figure 8. The dispersion value of these curves was assumed considering existing fragility data on unitized curtain walls (Memari et al. 2011). This comparison highlights that, while damage initiates earlier in the configuration with limited frame displacement capacity (lower drift values), the ultimate failure of the façade system occurs at similar high levels of drift ratios in both cases.

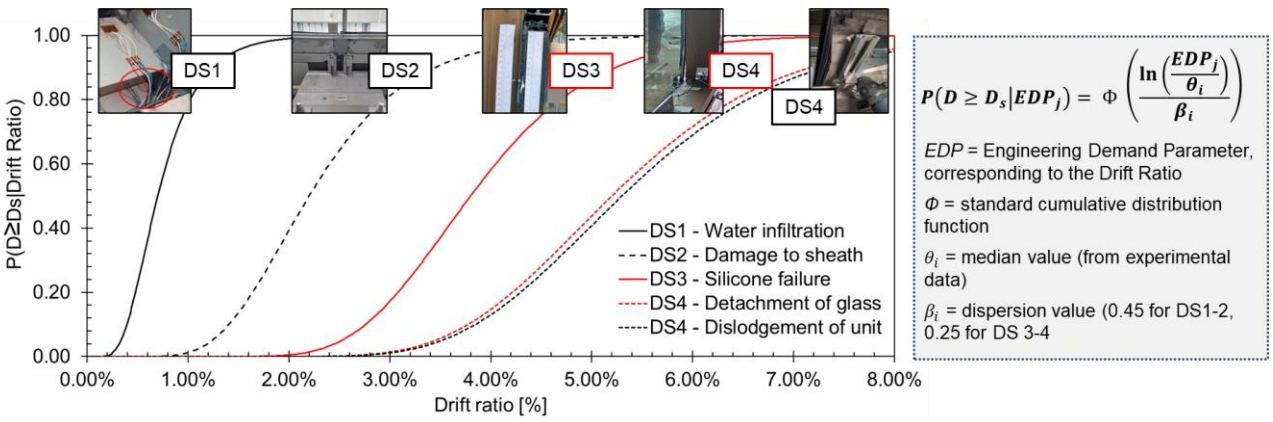

Figure 8. Damage states of SSG unitized curtain walls.

5. Conclusions

This paper has presented the key findings of experimental testing on structural silicone glazed facades, a common system in unitized curtain walls known for its potential to enhance seismic resilience. The investigation of expected damage states in façade systems involved full-scale seismic testing on specimens at the Permasteelisa testing facility in Vittorio Veneto, Italy. The experiments encompassed various specimen configurations with differing glass, pane and silicone joint dimensions, frame displacement capacity and

loading types, including in-plane displacement-controlled Crescendo tests, earthquake simulations and monotonic testing. This paper provided an overview of the test setup and program, as well as the initial analysis of sensor data and damage observations. The results highlighted several key points: (i) the ability of the façade system to withstand high drift ratios (>3% drift ratio) before potential failure occurred (>5% drift ratio); (ii) the influence of joint aspect ratio variations on panel movements, with lower aspect ratios leading to higher overall glass panel rotation; (iii) the significant influence of frame design on the behavior of the system and damage mechanisms during earthquakes. While further insights are anticipated through additional data analysis, post-processing is ongoing to provide a more comprehensive understanding of the impact of aspect ratios on the response of the system and overall damage states.

6. Acknowledgements

This study has received funding from the European Union's Horizon 2020 research and innovation programme under the Marie Skłodowska-Curie grant agreement No. 101029605 (H2020-MSCA-IF-2020 - SAFE-FACE - Seismic SAFety and Energy efficiency: Integrated technologies and multi-criteria performance-based design for building FACadEs) for Simona Bianchi. The authors also acknowledge the valuable contribution and support provided by Matteo Dazzan, Test & Lab specialist, Gianluca Casagrande, I&T specialist of the experimental measurement acquisition system and all the Test&Lab employees.

7. References

Arifin F.A., Sullivan T.J., Dhakal R.P. (2020). Experimental investigation into the seismic fragility of a commercial glazing system, *Bulletin of New Zealand Society for Earthquake Engineering*, 15(3): 144-149.

Baird A., Palermo A., Pampanin S. (2011). Facade damage assessment of multi-storey buildings in the 2011 Christchurch earthquake, *Bulletin of New Zealand Society for Earthquake Engineering*, 44(4): 368-376.

Bianchi S., Pampanin S. (2022). Fragility Functions for Architectural Nonstructural Components, *ASCE Journal of Structural Engineering*, 148(10).

Bianchi S., Lori G., Hayez V., Schipper R., Pampanin S., Overend M., Manara G., Klein T. (2022). Seismic testing and multi-performance evaluation of full-scale unitized curtain walls: research overview and preliminary results, *Proceedings of the* 5th *International Workshop on the Seismic Performance of Non-Structural Elements (SPONSE)*, Stanford, United States.

Broker K., Fisher S., Memari A. (2012). Seismic Racking Test Evaluation of Silicone Used in a Four-Sided Structural Sealant Glazed Curtain Wall System, *Journal of ASTM International*, 9(3):104144.

Hayez V., Bianchi S., Lori G., Feng J., Kimberlaind J. (2023). Performance of silicone bonded facades during seismic events. *Proceedings of the 2023 Glass Performance Days*, Tampere, Finland.

Huang B., Chen S., Lu W., Mosalam K.M. (2017). Seismic demand and experimental evaluation of the nonstructural building curtain wall: A review. *Soil Dynamics and Earthquake Engineering*, 100: 16–33.

Kimberlain J., Hayez V., Feng J., Mirgon M. (2022) SSG and Seismic Design Boundaries in Advanced Modeling, *Proceedings of Facade Tectonics 2022 World Congress*, Los Angeles, United States.

Lu W., Huang B., Mosalam K.M., Chen S. (2016). Experimental evalulation of a glass curtain wall of a tall building, *Earthquake Engineering Structural Dynamics*, 45(7): 1185-1205.

Memari, A.M. (2011). *Racking test evaluation of EN-WALL 7250 unitized curtain wall system with 3M™ VHB™ structural glazing tape*. Pennsylvania State University, United States.

Memari A.M., O'Brien W.C., Hartman K.J., Kremer P.A., Behr R A. (2011). *Architectural glass seismic behavior fragility curve development*. Background Document FEMA P-58/BD-3.9.1. Applied Technology Council, Redwood City, United States.

Miranda E., Mosqueda G., Retamales R., Pekcan G. (2010). Performance of nonstructural components during the 27 February 2010 Chile earthquake. *Earthquake Spectra*, 28(S1): S453-S471.

Nuñez Enriquez D.A. (2022). *Seismic Performance of Glazed Curtain Walls Connections: Experimental Testing and Finite Element Modelling*, Master Thesis of Civil Engineering, Delft University of Technology.

Zarghamee M.S., Schwartz T.A., Gladstone M. (1996). Seismic behavior of structural silicone glazing. *Science and technology of building seals, sealants, glazing and waterproofing*, Vol. 6, ASTMSTP 1286, James C. Meyers ed., American Society for Testing and Materials, West Conshohocken.